Journal of Materials Chemistry A

Accepted Manuscript

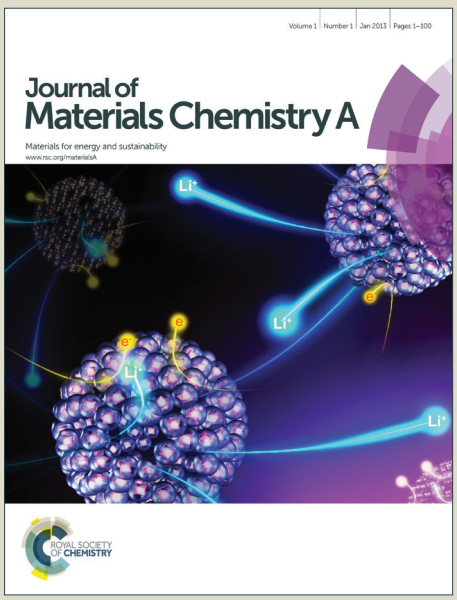

ROYAL SOCIETY OF CHEMISTRY

www.rsc.org/materialsA

ARTICLE TYPE www.rsc.org/xxxxxx | XXXXXXXX

Highly Selective and Efficient Heavy Metal Capture with Polysulfide Intercalated Layered Double Hydroxides

Shulan Ma,[a,b] Qingmei Chen,[a] Hao Li,[b] Pengli Wang,[b] Saiful M. Islam,[b] Qingyang Gu,[a] Xiaojing Yang[a] and Mercouri G. Kanatzidis[b,*]

Received (in XXX, XXX) Xth XXXXXXXXX 200X, Accepted Xth XXXXXXXXX 200X
First published on the web Xth XXXXXXXXX 200X
DOI: 10.1039/b000000x

The polysulfide $[S_x]^{2-}$ (x = 2, 4) species were intercalated into magnesium-aluminium layered double hydroxide (MgAl-LDH) by a $[S_x]^{2-}/NO_3^-$ anion-exchange reaction. The resulting S_x-LDH materials exhibit excellent affinity and selectivity for heavy metal ions such as Cu^{2+}, Ag^+ and Hg^{2+}. For the highly toxic Hg^{2+}, the distribution coefficient K_d values can reach ~10^7 mL/g. The S_x-LDH materials rapidly reduce the concentrations of Hg^{2+} and Ag^+ ions in testing solutions from ppm levels to trace levels of ≤ 1 ppb. A larger series of metal ions were investigated and the selectivity order of Ni^{2+}, Co^{2+} << Zn^{2+}, Pb^{2+} < Cd^{2+} < Cu^{2+}, Ag^+, Hg^{2+} was observed. The S_x-LDH materials show higher selectivity for Cu^{2+}/Zn^2 compared to Co^{2+}/Ni^{2+}, providing good separation for these transition metal ions. After ion capture, the LDH hybrid materials retained the original hexagonal prismatic shape and showed good stability under acidic conditions (pH ~ 3). The adsorption process of the metals occurs *via* M-S bonding. The enhanced environmental stability of the $[S_x]^{2-}$ groups provided by the LDH protective space, the confinement effect offered by the LDH layers, along with the easy accessibility of polysulfide ions to metal ions enable the high capture ability and excellent selectivity. The S_x-LDH materials are thus promising as superior sorbents for the decontamination of polluted water.

1. Introduction

The contamination of water by heavy metals has been an increasingly important issue in separation science and environmental remediation. The prominent heavy metal pollutants such as Hg^{2+}, Pb^{2+} and Cd^{2+} in some natural water sources and industrial waste water constitute a threat for humans and other species.[1-3] Ion exchange and chemical precipitation are traditional methods for removing these heavy metals.[4, 5] However, effective removal of heavy metal ions at low metal concentrations remains a great challenge.[6] Precipitation methods with sulfide ions cannot reduce the concentrations of heavy metals below acceptable drinking levels.[7] Thus, new and highly efficient adsorbents and methodologies need to be developed.

Selective metal adsorption on suitable substrate materials is considered one of the most economical methods of removal or recovery.[8] Natural adsorbents such as clays[9,10] and zeolites[11] have been commonly employed because of their high surface area, hydrophilic character and low cost. These materials, however, suffer from low selectivity and weak affinity for heavy metal ions. Alternatively, sulfide-based materials[12-16] seem to be effective for heavy metal remediation, as the high affinity of soft Lewis basic frameworks for the soft Lewis acids (e.g. Hg^{2+}) is innate to these materials. Mineral sulfides, such as FeS_2, have the disadvantage of adsorbing metal ions only on their surface, due to their dense structures.[17-19] Therefore, the integration of certain inorganic layered compounds with sulfide-based materials may result in novel families of adsorbents.

Several functionalized layered materials have shown efficiency for heavy metal remediation.[20-23] Our group reported synthetic layered sulfides, such as $K_{2x}Mn_xSn_{3-x}S_6$ (KMS)[24-29] or $H_{2x}Mn_xSn_{3-x}S_6$,[30] with good ability for removing heavy metal ions. These materials operate under the soft-hard Lewis acid-base paradigm for the metal selectivity. Considering the polysulfides $[S_x]^{2-}$ can form strong covalent bonds with soft heavy metals[31-38] or with some presumed "hard" cations such as uranyl,[31] their utility to sequester metals is worthy of investigation. However, the common polysulfide compounds such as K_2S_x are water-soluble and cannot act as heterogeneous sorbents in aqueous systems. Furthermore, the application of polysulfide compounds is limited due to their sensitivity to atmospheric oxygen.[39]

The layered double hydroxides (LDHs), known a type of anionic clay, are unique among layered compounds, because they have positively-charged host layers and counter-anions in the interlayer. Thanks to their excellent exchangeability, LDHs can work as precursors to introduce other species to fabricate hybrid materials, which reveal important applications on adsorption,[40,41] catalysis,[42-45] separation science,[46-49] storage and triggered release of functional guests,[50-53] optical materials,[54] etc. LDH materials have been studied for the removal of heavy metal ions, but in general they exhibit low selectivity.[55-58] The most effective means of removing metal ions from soluton is through the formation of M-S bonds. Considering the attractive features of LDHs such as high surface area, facile ion-exchange, hydrophilic

character, they may be readily functionalized with metal-binding polysulfide ions. The water-soluble polysulfide anions can be introduced into the interlayer, forming layered solids that can be used in heterogeneous adsorption. LDH intercalated with mercaptocarboxylic acid (with S-H group) was reported to remove Hg^{2+},[59] but with moderate efficiency possibly due to the steric hindrance of carboxylic groups. The LDH galleries provide a protective space, which offers the inserted $[S_x]^{2-}$ groups enhanced environmental stability. Therefore, the incorporation of $[S_x]^{2-}$ groups into LDH offers new hybrids that act as selective scavengers for heavy metals

Herein, we report the intercalation of the polysulfides of K_2S_x [x = 2, 4] into a NO_3^- type MgAl-LDH. When separating Cu^{2+}, Hg^{2+} and Ag^+ from complex mixtures of metals, these materials (referred to as S_x-LDH) showed excellent removal capacity (~686 mg/g for Hg^{2+}) and high selectivity (K_d for Hg^{2+} can achieve ~10^7 mL/g) toward heavy metals. This places them among the top materials known for heavy metal removal. More importantly, the ability of reducing heavy metal pollutants (Hg^{2+} and Ag^+) of any concentration (even very low ppm level) down to ppb makes these intercalated polysulfides promising for environmental applications.

2. Experimental section

2.1 Materials.

The MgAl–CO_3–LDH was prepared by the HMT (hexamethylenetetramine) hydrolysis method[60,61] as we previously reported.[62] The MgAl–NO_3–LDH was prepared through NO_3^-/CO_3^{2-} anion exchange reaction.[61] The polysulfides of K_2S_x (x = 2, 4) were prepared by the reaction of K and S in liquid ammonia as described previously.[37] The $[S_x]^{2-}$ anions were exchanged with NO_3^- to get S_x-LDH. Typically, 0.2 g NO_3–LDH and 0.2 g K_2S_x (x = 2 or 4) was first put into 20 mL glass vial inside a glovebox. The vials were removed from the glovebox and 8 ml dispersed degassed deionized water was added. The obtained suspension was sealed and left for reaction at ambient temperature for 24 h. The resulting S_x–LDH solids were filtered, washed with deionized water and then acetone, finally air-dried.

2.2 Heavy metal uptake experiments.

The heavy metal uptake from aqueous solutions of various concentrations (10 and 20 ppm, 2.5 and 10 mM) was studied using a batch method. The solid sorbents were immerged with the solution of $M(NO_3)_m$ (M = Co^{2+}, Ni^{2+}, Cu^{2+}, Zn^{2+}, Ag^+, Pb^{2+}, Cd^{2+}, Hg^{2+}) with intermittent shaking for 3 h, 6 h, 24 h and sometimes 3 days.

For distinguishing Hg^{2+} from Ag^+ clearly, an experiment containing only Ag^+ and Hg^{2+} in solution was carried out. A concentration of ~20 ppm for each ion (40 ppm for Ag^++Hg^{2+}) mixed with small quantity of S_x-LDH (0.001 and 0.002 g) was used that was adequate to pick up one of the two ions but not both.

After mixing the solid sorbents with the solutions for a certain time, a filtration was performed and the concentrations of metal ions in the supernatant solution (separated by centrifugation) were determined using inductively coupled plasma-atomic emission spectroscopy (ICP-AES) and inductively coupled plasma-mass spectroscopy (ICP-MS) for extra low ion concentration. The adsorption capacity was evaluated from the difference of metal concentrations in the mother and supernatant solutions.

The distribution coefficient K_d used for determining the selectivity of S_x-LDH for heavy metals is given by the equation $K_d = (V[(C_0 - C_f)/C_f])/m$, where C_0 and C_f are respectively the initial and local concentration of M^{n+} (ppm) after the contact, V is the volume (mL) of the testing solution, and m is the amount of the solid sorbent (g) used in the experiment.[24] Our experiments were performed with V:m ratios of 500-30000 mL/g at ambient temperature.

2.3 Characterization techniques.

The powder X-ray diffraction (XRD) patterns were collected using a Phillips X' pert Pro MPD diffractometer with Cu-Kα radiation, at room temperature, with step size of 0.0167 °, scan time of 15 s per step, and 2θ ranging from 4.5 to 70 °. The generator setting was 40 kV and 40 mA. Fourier transformed infrared (FT–IR) spectra of the samples were recorded on a Nicolet-380 Fourier-Transform infrared spectrometer using the KBr pellet method. Raman spectra were taken on a microscopic confocal Raman spectrometer, using a 633 nm He–Ne laser. Scanning electron microscope (SEM) measurements were carried out using a Hitachi S-4800 microscope at 5.0 kV. The metal ion contents in solid samples were determined by inductively coupled plasma atomic emission spectroscopy (ICP-AES, Jarrel-ASH, ICAP-9000), and a 0.1 M HNO_3 solution was used to dissolve them. The metal ion concentrations in supernatant solution after adsorption experiment were measured using ICP-AES technique and for extra low concentrations the inductively coupled plasma-mass spectroscopy (ICP-MS, NexION 300X) was used. C, H and N contents of the solid samples were determined using an Elementar Vario EL elemental analyzer. The chemical formulas of the samples were calculated from the results of ICP and CHN analyses.

3. Results and Discussion

3.1 Synthesis and characterization of S_x-LDH materials.

The synthesis of polysulfide containing LDH materialswas accomplished via the ion-exchange reaction in eq. (1).

$$Mg_{0.66}Al_{0.34}(OH)_2(NO_3)_{0.34}\ xH_2O + 0.17K_2S_4 \rightarrow Mg_{0.66}Al_{0.34}(OH)_2(S_4)_{0.17}\ xH_2O + 0.34KNO_3 \quad \text{eq. (1)}$$

The exact molecular formulae of CO_3–LDH, NO_3–LDH, S_4-LDH and S_2-LDH (Table 1) were determined *via* ICP, CHN analysis and charge balance considerations. Compared with the NO_3-LDH precursor, it is clear that some adventitious CO_3^{2-} ions re-enter the structure, which is attributed to the very strong affinity of this ion for the LDH layers.[63] Based on the XRD data the small amount of CO_3^{2-} likely co-exists with $[S_x]^{2-}$ in the interlayer space and does not form a separate phase.

Fig.1A shows the XRD patterns of CO_3^{2-}– and NO_3^-–LDH precursors and the exchanged products. The sharp and symmetric features of the diffraction peaks indicate the high crystallinity of the samples. All compounds exhibit a series of strong basal (00*l*) Bragg reflections characteristic of a layered phase and a high degree of orientation. The *d* values of 0.76 and 0.89 nm (Fig. 1A-a,b) are characteristic of CO_3^{2-}– and NO_3^-–type LDHs. As shown in Fig. 1A-c, a series of strong (00*l*) reflections at 0.81, 0.40 and 0.22 nm for the S_4-LDH sample indicate a layered phase with basal spacing (d_{basal}) of 0.81 nm. Since the thickness of the LDH layer is 0.48 nm,[64] the gallery height can be estimated at ~ 0.33 nm (= 0.81 – 0.48). The small gallery height suggests a flat arrangement of the zig-zag polysulfide $[S_4]^{2-}$ group in the interlayer, as shown in Scheme 1.

S_2–LDH has a slightly shorter d_{basal} of 0.80 nm (Fig. 1A-d), consistent with the smaller size of $[S_2]^{2-}$. From the XRD patterns, it is apparent that the intercalation of the different anions shifts the position of the (00*l*) reflections, but the peak at *d* = 0.15 nm corresponding to the (110) plane in the 2D LDH sheets does not change. This indicates the stability of the brucite layers during the ion-exchange process, *i.e.* a topotactic ion-exchange, which is also supported by the SEM observation discussed later.

IR and Raman spectra (Fig. 1B and 2A) verify the formation of the intercalated compounds and their successful ion-exchange. In the IR spectra (Fig. 1B-a), the bands at 1354 and 780 cm^{-1} are the characteristic absorptions of CO_3-LDH.[60] After the treatment of the CO_3–LDH with $NaNO_3$ + HNO_3, the 1354 cm^{-1} band (CO_3^{2-}) disappears, and a strong band appears at 1384 cm^{-1} (Fig. 1B-b) corresponding to NO_3^- absorption. When the $[S_4]^{2-}$ anions are intercalated, the NO_3^- absorption at 1384 cm^{-1} becomes weak or negligible, consistent with a nearly complete exchange. Generally, small and highly charged anions preferentially occupy the LDH interlayer space.[39,63,65-67] Thus, the -2 charge of the polysulfide ion provides a strong driving force for the exchange over the singly charged nitrate. The bands at 681 and 445 cm^{-1} in NO_3-LDH (Fig. 1B-b) respectively assigned to ν(M–O) and δ(O–M–O) vibrations[68, 69] shift to 663 and 447 cm^{-1} (Fig. 1B-c) in S_4-LDH, possibly due to the effect of interlayer guest.

The S-S stretching vibrations occuring in the region of 477-486 cm^{-1} [70] in the IR spectra may overlap with the strong Mg(Al)–O vibrations appearing in the same range (Fig. 1B-c). Raman spectra, however, give better evidence for S-S bonds. From Fig. 2A-d, the bands at 228, 267, 434 and 484 cm^{-1} are consistent with the symmetric and asymmetric S−S vibrations of polysulfide anions.[70] After intercalation of $[S_x]^{2-}$ (Fig. 2A-e), the main vibration bands remain but with small shifts, reflecting the interaction of $[S_x]^{2-}$ with the LDH host layer. For K_2S_2 (Fig. 2A-b) and S_2-LDH (Fig. 2A-c), there is only one peak at 455 cm^{-1} consistent with one S-S bond. The different vibration bands in S_2-LDH and S_4-LDH showed the different groups in the interlayer of the composites.

The SEM observations (Fig. 2B-a) indicate the crystallites of NO_3–LDH have a hexagonal prismatic shape, retaining the morphology of the CO_3–LDH precursor.[60] After ion-exchange of NO_3^- with $[S_x]^{2-}$, the S_x-LDH crystallites fully maintained the hexagonal prismatic shape (Fig. 2B-e), confirming topotactic insertion of the polysulfide anions.

3.2 Heavy metal ion removal using S_x-LDH.

The uptake of heavy metal ions by S_x-LDH from aqueous solutions of various concentrations was studied with the batch method (*V*:*m* = 500-30000 mL/g, contact exposure time of 3-72 h, room temperature). The affinity of S_x-LDH for the metal ions is reflected in the distribution coefficient K_d values. At first, adsorption experiments with individual solutions of the ions Co^{2+}, Ni^{2+}, Cu^{2+}, Zn^{2+}, Ag^+, Pb^{2+}, Cd^{2+} and Hg^{2+} were performed. Subsequently, metal removal experiments using solutions containing all these ions simultaneously were carried out. We used three sets of metal ion concentrations: low values of 10 and 20 ppm for assessing the selectivity, and high value of 10 mM for assessing removal capacity. The *V*:*m* values varied from 500 to 30000 mL/g, with a solution volume (*V*) of 10 and 30 ml and solid mass (m) from 0.002 g to 0.035 g.

Table 2 summarizes the adsorption results of individual ions by the S_4-LDH. From this table, the general selectivity order for the eight ions is as follows Ni^{2+}, Co^{2+} < Zn^{2+}, Cd^{2+} << Cu^{2+}, Pb^{2+} << Hg^{2+}, Ag^+. The adsorption ability and selectivity toward Hg^{2+}/Ag^+ and Cu^{2+}/Pb^{2+} is much higher than all other ions. After 3 h of contact time, the concentrations of Hg^{2+}, Ag^+ decreased from the starting value of ~10 ppm to ≤1 ppb, with nearly 100 % removal achieved. At the same time, 75-80 % removal was observed for Cu^{2+} and Pb^{2+}. The adsorption selectivity for Zn^{2+} and Cd^{2+} was not high. Below we will discuss experiments using mixtures of all these ions where a much higher selectivity is observed.

The removal results from the solutions containing all ions (e.g. "mixed ion state") are shown in Table 3. The concentration of each ion in the starting solution was ~10 ppm. Using equal amount of 0.035 g S_4-LDH as in the single adsorption experiments, a selectivity order of Ni^{2+}, Co^{2+} << Zn^{2+}, Pb^{2+} < Cd^{2+} < Cu^{2+}, Ag^+, Hg^{2+} was observed, generally in agreement with those seen in single adsorption experiments, except for the different order seen among Cu^{2+}, Pb^{2+} and Cd^{2+}. Nearly all of the ions gave increased K_d values (Table 2 and 3): 4000 fold (= $9.5\times10^6/2.4\times10^3$) for Cu^{2+}, 4260 (= $1.3\times10^6/305$) fold for Zn^{2+}, 533 fold (= 1.6×10^6 / 3.0×10^3) for Pb^{2+}, and the biggest augmentation of 17420 (= $6.9\times10^6/396$) fold was observed for Cd^{2+}. We speculate that a cooperative interaction of various coexisting cations may be responsible for the increase. Another reason may be the acidity of the mixed solution (pH is ~3) resulting from the dissolution of all these salts. The acidity may affect the hydration of some cations to various degrees which may modulate the binding driving force with the $[S_x]^{2-}$ group.

From Table 3 and Table S1 (Supporting Information), we can see that the present materials (0.01-0.035 g S_4-LDH and S_2-LDH) can rapidly reduce the concentrations of Cu^{2+}, Hg^{2+} and Ag^+ ions to a very low level. This, however, makes it difficult to carry out experiments to assess the potential to separate these ions from one another when all are present in

solution. In order to distinguish the cations more clearly, we used much lower amounts of S_4-LDH (0.002 g) and S_2-LDH (0.005 g). For S_4-LDH, when using 0.002 g, a clear order of Cu^{2+} << Ag^+, Hg^{2+} emerges, and 0.005 g and 0.01 g show an order of Cd^{2+}, Pb^{2+} < Cu^{2+} << Ag^+, Hg^{2+}. When using 0.02 g, an order of Zn^{2+} < Cd^{2+}, Pb^{2+}< Cu^{2+} < Ag^+, Hg^{2+} was observed. Using an amount of 0.035 g S_4-LDH gave improved selectivity to Zn^{2+} and Cd^{2+} while those for other ions hardly changed, giving a final order of Ni^{2+}, Co^{2+} < Zn^{2+} < Pb^{2+} < Cd^{2+} < Cu^{2+} < Ag^+, Hg^{2+} (Table 3). For S_2-LDH (Table S1, Supporting Information), a similar selectivity order of Ni^{2+}, Co^{2+} < Zn^{2+} < Cd^{2+} < Pb^{2+}, Cu^{2+} < Ag^+, Hg^{2+} was observed, with only a small difference for Cd^{2+} and Pb^{2+}.

From Table 3, we can see that when using 0.02-0.035 g S_4-LDH (3 h contact time), >99% removal was observed for Cu^{2+}, Zn^{2+}, Ag^+, Pb^{2+}, Cd^{2+} and Hg^{2+} (actually 100% for Hg^{2+}, Ag^+ and Cu^{2+}). Using lower amount of S_4-LDH (e.g. 0.01 g) gave sharply decreased removal for Zn^{2+} (~20%) while even lower amounts (e.g. 0.005 g) gave only 1 % removal. These small amounts, however, could still remove Ag^+/Hg^{2+} with ~100 % and Cu^{2+} with 80 % efficiency. It should be noted that the removal of Co^{2+} and Ni^{2+} was negligible when using 0.01 g S_4-LDH and only 4-10 % when using 0.02-0.035 g. The reasons for the much lower removal ability of S_x-LDH for Co^{2+} and Ni^{2+} relative to Cu^{2+} and Zn^{2+} are not clear.

The higher preference of S_x-LDH for Hg^{2+}/Ag^+ over Pb^{2+}/Cd^{2+} is reflected in the K_d^{Hg} and K_d^{Ag} values which are 10-100 times higher than those for Pb^{2+} and Cd^{2+}. This shows that S_x-LDH is very selective for cations with high Lewis acid softness (*i.e.* Hg^{2+}/Ag^+ *vs.* Pb^{2+}/ Cd^{2+}).

It is noted that for the highly toxic Hg^{2+}, the K_d values can reach ~10^7 mL/g, matching or exceeding those reported for commercial resins (~10^4–5.1×10^5 mL/g),[71,72] the silane chelating fibers (3.0×10^5–3.8×10^6 mL/g),[73] chalcogel-1 (9.2×10^6–1.6×10^7)[35] and mesoporous thiol-functionalized silicates (3.4×10^5–1.0×10^8 mL/g).[14,71,74] While the S_x-LDH materials form direct M-S bonds with the metal ions, the functionalized silica sorbents generally need incorporation of custom designed sulfur containing organic functional groups.

Clearly, the present materials can rapidly reduce the concentration of soft ions to very low levels. Namely, the S_x-LDH can decrease Ag^+, Hg^{2+} and Cu^{2+} from 10 ppm to ≤ 1 ppb very fast (Table 2, 3 and Table S1, Supporting Information). The reduced Hg^{2+} concentration was always lower than 1 ppb, well below the acceptable level in drinking water (2 ppb).[75] These results indicate the potential of S_x-LDH as a kind of highly effective filters for immediate decontamination of water polluted with heavy metal ions especially Hg^{2+}. Remarkably, enormous K_d values for Hg^{2+} and Ag^+ were observed regardless of the S_x-LDH amount used, consistent with a tremendous affinity for these ions.

3.3 Relative selectivity for Ag^+ and Hg^{2+}.

Generally, it is difficult to remove Hg^{2+} selectively from a mixture containing Ag^+ ions. The ability to separate these two ions from one another is important because such a challenging problem is often encountered in mining operations of precious metals. From Tables 2 and 3 (regarding S_4-LDH) and Table S1 (Supporting Information, regarding S_2-LDH), we can see that Ag^+ and Hg^{2+} are so similar in their reactivity that they cannot be selectively separated using the S_x-LDH under the employed operating conditions. In an attempt at selectively separating Ag^+ from Hg^{2+}, we used a solution containing Ag^+ and Hg^{2+} in 20 ppm concentration for each ion (no other cations were present). Then, a small quantity of S_x-LDH (0.001 g and 0.002g) was used which was sufficient to pick up only one of the two ions. From Table 4, we can see that when using 0.001 g S_4-LDH, the K_d for Hg^{2+} is nearly 50 times greater than that for Ag^+, while this drops to only 2.6 fold when using 0.002 g of solid. This means the S_4-LDH has somewhat higher selectivity for Hg^{2+} than for Ag^+. Similarly, S_2-LDH also has higher selectivity toward Hg^{2+} (Table 4). For S_2-LDH, the K_d of Hg^{2+} was 36 times that of Ag^+ when using 0.001 g of solid and 7 fold when using 0.002 g of solid. Therefore a careful dosing of S_x-LDH material is important for the successful separation of these two ions.

3.4 Uptake capacity toward metal ions.

In the single ion removal experiments described above, the molar ratio of each ion to the bonding sites ($[S_x]^{2-}$) in S_x-LDH materials is about 0.05, and in the mixed adsorption (all ions together), the molar ratio of all ions to the bonding sites is about 0.5. Therefore, the solid material used could quantitatively absorb the ions without saturating its exchange sites. In order to check the maximum capacity, we increased the solution concentration to 2.5-10 mM and the molar ratios to 0.7-3. As shown in Table 5, taking S_2-LDH as an example, the uptakes for Hg^{2+}, Pb^{2+}, Ag^+ and Zn^{2+} are respectively 686, 483, 383, and 145 mg/g, corresponding to 3.42, 2.33, 3.55 and 2.22 mmol/g. For Cu^{2+}, the uptake is 127 mg/g or 2.01 mmol/g (Table 5). Even when using a smaller concentration of 2.5 mM and mixing the Hg^{2+}, Ag^+ and Cu^{2+} the material still showed a high level of removal of 441, 254, and 172 mg/g (Table S2, Supporting Information). It suggests that S_x-LDH can remove large amounts of heavy metal ions.

3.5 Structural characterization and morphologies of solids after metal adsorption.

As shown in Fig. 3, in the case of smaller ion concentrations of 10 ppm, after adsorption the samples show increased basal spacings (d_{basal}, by XRD) of 0.88/0.89, 0.82/0.83 nm. The Bragg peak at 0.76 nm corresponds to CO_3-LDH, resulting from adventitious CO_3^{2-} anions (from air and water). The d_{basal} values of 0.88/0.89, 0.82/0.83 nm are attributed to various coordination motifs of metal ions to the $[S_x]^{2-}$ groups. It is noted that for Ag^+ containing samples, the d_{basal} values of 0.80 nm and 0.76 nm are unchanged suggesting that insertion in low concentrations and binding to $[S_x]^{2-}$ does not cause a significant disruption in the interlayer space. When a large ion concentration of 10 mM was used, as shown in Fig. 4e, the sample exhibited three d_{basal} values of 0.88, 0.82 and 0.78 nm.

SEM images of the samples after metal ion adsorption show retention of the hexagonal prismatic shape, Fig. 5. Although the Hg^{2+} solution is acidic with pH values of ~3, the S_x-LDH intercalates still kept the hexagonal prismatic morphology (Fig. 5h,h'), indicating considerable stability in acidic

environments.

Based on CHN analyses, the solids after metal adsorption had nearly no NO_3^- (no N content detected), but they had traces adventitious CO_3^{2-} (~1-2 % C content). The presence of CO_3^{2-} ions is confirmed by the FT-IR spectra (Fig. 6). The bands at 1358-1360 cm^{-1} and 771-776 cm^{-1} are the characteristic absorptions of CO_3-LDH,[60] as found in Fig. 1B-a. Compared with the strong CO_3^{2-} vibration the NO_3^- adsorption is very weak, consistent with its trace content. Combining the XRD, IR data and CHN analyses, a possible structural arrangement is shown in Scheme 1b. CO_3^{2-} exists mainly as a distinct phase with basal spacing of 0.76/0.78 nm, while any trace NO_3^- may co-exist with M-S_x phases with a flat-lying conformation in the interlayer space.

The adsorption of metal ions proceeds by complexation with the interlayer $[S_x]^{2-}$ group to form polysulfide complexes.[76, 77] In a way, the intercalated polysulfide species can act as a second host to incoming metal ions. Another important point in the IR spectra is the shift of the ν(M-O) vibrations from 663 to 681-683 cm^{-1} after metal adsorption (Fig. 6). From Fig. 1B-b, we know in pristine NO_3-LDH the ν(M-O) vibration also appeared at 681 cm^{-1}. This indicates that the binding of metal ions to the polysulfide anions converts the S_x-LDH back to NO_3-LDH plus associated MS_x species as a second phase. Additionally, the unchanged band at 447/448 cm^{-1} assigned to δ(O–M–O) vibrations[68] indicates the total stability of the LDH layer after the adsorption. The Raman spectra (Fig. 2A-g,h) after S_4-LDH adsorbed metal ions (10 ppm) show the polysulfide S-S vibrations in the range of 151-475 cm^{-1}. The slight shift of the peaks relative to the metal-free S_4-LDH reflects the interaction of the metal ions with the polysulfide.

Depending on the S_4-LDH/M ratio used the above observations may be rationalized as follows.

1) In the very low metal concentration limit, where the LDH-S_x material is in large excess, the following reaction scheme appears to operate:

$$LDH(S_x)+M(NO_3)_2 \rightarrow LDH(NO_3^-)_m([M^{2+}(S_x^{2-})_2]^{2-})_n \quad \text{eq. (2)}$$

In this case, adduct formation occurs and the various m and n values result in different basal spacings as observed in the XRD patterns of the samples (Fig. 3). This model is shown in Scheme 1b.

2) In the high metal concentration limit the reactions are stoichiometric and may be represented under the double metathesis scheme shown below:

$$LDH(S_x)+M(NO_3)_2 \rightarrow LDH(NO_3)+MS_x \quad \text{eq. (3)}$$

In this case, two phases LDH(NO_3) and MS_x are formed. The MS_x phase is amorphous revealing no signatures in the XRD patterns. In both of the above cases, NO_3^- anions are present as verified by the IR adsorption at 1384 cm^{-1}.

4. Conclusions

The polysulfide $[S_x]^{2-}$ (x = 2, 4) ions intercalate in a straightforward manner into the Mg/Al layered double hydroxides (MgAl-LDH) by anion-exchange. The basal spacings of the as-formed nanocomposites S_4–LDH and S_2–LDH suggest a flat lying arrangement in the interlayer. The S_x-LDH intercalates are remarkably selective toward heavy metal ions in aqueous solution. The materials display significant ion uptake and excellent selectivity for Cu^{2+}, Ag^+ and Hg^{2+}. A selectivity order of $Ni^{2+} < Co^{2+} < Zn^{2+} < Pb^{2+} < Cd^{2+} < Cu^{2+} < Ag^+$, Hg^{2+} was obtained. For the highly toxic Hg^{2+}, K_d values of ~10^7 mL/g were observed, comparable to or better than the previously reported materials. The S_x-LDH materials can quickly reduce Ag^+ and Hg^{2+} concentrations from 10 ppm to ≤1 ppb levels, well below the acceptable limits for drinking water. In mixed solutions with multiple kinds of ions present, even higher K_d values were observed compared to the individual ions solutions. The formation of M-S bonds between the intercalated polysulfides and the metal ions accouts for the effective removal for the heavy metals. After intercalation and metal loading, the materials retain their well-defined hexagonal prismatic shape, even under mild acidic conditions (pH~3), indicating good chemical stability. Because of their advantages, these LDH/polysulfide composite materials may be excellent candidates for use in highly efficient filters for rapid decontamination of water from heavy metal ions.

Acknowledgments.

This work is supported by the National Science Foundations of China 21271028 and 51272030. At Northwestern University financial support from the National Science Foundation (Grant DMR-1104965) is gratefully acknowledged.

Notes and references

[a] *Beijing Key Laboratory of Energy Conversion and Storage Materials, College of Chemistry, Beijing Normal University, Beijing 100875, China. Fax: 86 10 5880 2075; Tel: 86 10 5880 7524; E-mail: mashulan@bnu.edu.cn*

[b] *Department of Chemistry, Northwestern University, 2145 Sheridan Road, Evanston, IL 60208, USA. Fax: 01 8474915937; Tel: 01 8474671541; E-mail: m-kanatzidis@northwestern.edu*

† Electronic Supplementary Information (ESI) available: adsorptive capacity and selectivity of S_2-LDH toward 10 ppm metal ions, adsorptive capacity of S_4-LDH toward 2.5 mM metal ions. See DOI: 10.1039/b000000x/

1 A. P. Carnizello, L. Marcal, P. S. Calefi, E. J. Nassar, K. J. Ciuffi, R. Trujillano, M. A. Vicente, S. A. Korili and A. Gil, *J. Chem. Eng. Data*, 2009, 54, 241-247.

2. M. A. Shannon, P. W. Bohn, M. Elimelech, J. G. Georgiadis, B. J. Marinas and A. M. Mayes, *Nature*, 2008, 452, 301-310.

3. R. P. Schwarzenbach, B. I. Escher, K. Fenner, T. B. Hofstetter, C. A. Johnson, U. von Gunten and B. Wehrli, *Science*, 2006, 313, 1072-1077.

4. I. H. Lee, Y. C. Kuan and J. M. Chern, *J. Hazard. Mater.*, 2006, 138, 549-559.

5. B. R. Kim, W. A. Gaines, M. J. Szafranski, E. F. Bernath and A. M. Miles, *J Environ Eng-Asce*, 2002, 128, 612-623.

6. K. G. Bhattacharyya and S. Sen Gupta, *Sep. Purif. Technol.*, 2006, 50, 388-397.

7. D. R. Tonini, D. A. Gauvin, R. W. Soffel and W. P. Freeman, *Environ. Prog.*, 2003, 22, 167-173.
8. R. M. Schneider, C. F. Cavalin, M. A. S. D. Barros and C. R. G. Tavares, *Chem. Eng. J.*, 2007, 132, 355-362.
9. A. Benhammou, A. Yaacoubi, L. Nibou and B. Tanouti, *J. Colloid Interface Sci.*, 2005, 282, 320-326.
10. Y. El Mouzdahir, A. Elmchaouri, R. Mahboub, A. ElAnssari, A. Gil, S. A. Korili and M. A. Vicente, *Appl. Clay Sci.*, 2007, 35, 47-58.
11. G. Blanchard, M. Maunaye and G. Martin, *Water Res.*, 1984, 18, 1501-1507.
12. L. Mercier and T. J. Pinnavaia, *Adv. Mater.*, 1997, 9, 500-&.
13. J. Brown, L. Mercier and T. J. Pinnavaia, *Chem. Commun.*, 1999, 69-70.
14. X. Feng, G. E. Fryxell, L. Q. Wang, A. Y. Kim, J. Liu and K. M. Kemner, *Science*, 1997, 276, 923-926.
15. Y. S. Shin, G. Fryxell, W. Y. Um, K. Parker, S. V. Mattigod and R. Skaggs, *Adv. Funct. Mater.*, 2007, 17, 2897-2901.
16. B. J. Riley, J. Chun, J. V. Ryan, J. Matyáš, X. S. Li, D. W. Matson, S. K. Sundaram, D. M. Strachan and J. D. Vienna, *RSC Adv.*, 2011, 1, 1704-1715.
17. D. Borah and K. Senapati, *Fuel*, 2006, 85, 1929-1934.
18. A. Ozverdi and M. Erdem, *J. Hazard. Mater.*, 2006, 137, 626-632.
19. M. Erdem and A. Ozverdi, *Sep. Purif. Technol.*, 2006, 51, 240-246.
20. A. De Martino, M. Iorio and R. Capasso, *Chemosphere*, 2013, 92, 1436-1441.
21. N. Gutierrez, E. Ramos, C. Contreras and M. Olguin, *Revista Mexicana De Fisica*, 2009, 55, 135-138.
22. R. Rojas, M. R. Perez, E. M. Erro, P. I. Ortiz, M. A. Ulibarri and C. E. Giacomelli, *J. Colloid Interface Sci.*, 2009, 331, 425-431.
23. H. Yamada, K. Tamura, Y. Watanabe, N. Iyi and K. Morimoto, *Sci. Technol. Adv. Mater.*, 2011, 12.
24. M. J. Manos, N. Ding and M. G. Kanatzidis, *P Natl Acad Sci USA*, 2008, 105, 3696-3699.
25. M. J. Manos and M. G. Kanatzidis, *Chem-Eur. J.*, 2009, 15, 4779-4784.
26. M. J. Manos, C. D. Malliakas and M. G. Kanatzidis, *Chem-Eur. J.*, 2007, 13, 51-58.
27. M. J. Manos and M. G. Kanatzidis, *J. Am. Chem. Soc.*, 2009, 131, 6599-6607.
28. M. J. Manos and M. G. Kanatzidis, *J. Am. Chem. Soc.*, 2012, 134, 16441-16446.
29. J. L. Mertz, Z. H. Fard, C. D. Malliakas, M. J. Manos and M. G. Kanatzidis, *Chem. Mater.*, 2013, 25, 2116-2127.
30. M. J. Manos, V. G. Petkov and M. G. Kanatzidis, *Adv. Funct. Mater.*, 2009, 19, 1087-1092.
31. A. C. Sutorik and M. G. Kanatzidis, *J. Am. Chem. Soc.*, 1997, 119, 7901-7902.
32. A. Muller, E. Krickemeyer, V. Wittneben, H. Bogge and M. Lemke, *Angew. Chem. Int. Ed.*, 1991, 30, 1512-1514.
33. M. Shafaei-Fallah, J. Q. He, A. Rothenberger and M. G. Kanatzidis, *J. Am. Chem. Soc.*, 2011, 133, 1200-1202.
34. N. Ding and M. G. Kanatzidis, *Nature Chem.*, 2010, 2, 187-191.
35. S. Bag, P. N. Trikalitis, P. J. Chupas, G. S. Armatas and M. G. Kanatzidis, *Science*, 2007, 317, 490-493.
36. S. Bag, A. F. Gaudette, M. E. Bussell and M. G. Kanatzidis, *Nature Chem.*, 2009, 1, 217-224.
37. Y. Oh, C. D. Morris and M. G. Kanatzidis, *J. Am. Chem. Soc.*, 2012, 134, 14604-14608.
38. M. J. Manos, K. Chrissafis and M. G. Kanatzidis, *J. Am. Chem. Soc.*, 2006, 128, 8875-8883.
39. M. Ogawa and F. Saito, *Chem. Lett.*, 2004, 33, 1030-1031.
40. Y. Gao, Z. Zhang, J. Wu, X. Yi, A. Zheng, A. Umar, D. O'Hare and Q. Wang, *J. Mater. Chem. A*, 2013, 1, 12782-12790.
41. Y. Tokudome, N. Tarutani, K. Nakanishi and M. Takahashi, *J. Mater. Chem. A*, 2013, 1, 7702-7708.
42. F. Cavani, F. Trifiro and A. Vaccari, *Catal. Today*, 1991, 11, 173-301.
43. B. Sels, D. De Vos, M. Buntinx, F. Pierard, A. Kirsch-De Mesmaeker and P. Jacobs, *Nature*, 1999, 400, 855-857.
44. H. Zhang, G. Zhang, X. Bi and X. Chen, *J. Mater. Chem. A*, 2013, 1, 5934-5942.
45. N. Baliarsingh, L. Mohapatra and K. Parida, *J. Mater. Chem. A*, 2013, 1, 4236-4243.
46. M. R. Perez, I. Pavlovic, C. Barriga, J. Cornejo, M. C. Hermosin and M. A. Ulibari, *Appl. Clay Sci.*,2006, 32, 245-251.
47. S. L. Ma, C. H. Fan, L. Du, G. L. Huang, X. J. Yang, W. P. Tang, Y. Makita and K. Ooi, *Chem. Mater.*, 2009, 21, 3602-3610.
48. X.-L. Wu, L. Wang, C.-L. Chen, A.-W. Xu and X.-K. Wang, *J. Mater. Chem.*, 2011, 21, 17353-17359.
49. C. Gao, X.-Y. Yu, T. Luo, Y. Jia, B. Sun, J.-H. Liu and X.-J. Huang, *J. Mater. Chem. A*, 2014, 2, 2119-2128.
50. S. Bonnet, C. Forano, A. deRoy, J. P. Besse, P. Maillard and M. Momenteau, *Chem. Mater.*, 1996, 8, 1962-1968.
51. J. Tronto, K. C. Sanchez, E. L. Crepaldi, Z. Naal, S. I. Klein and J. B. Valim, *J. Phys. Chem. Solids*, 2004, 65, 493-498.
52. E. Geraud, V. Prevot, C. Forano and C. Mousty, *Chem.l Commu.* 2008, 1554-1556.
53. J.-H. Choy, S.-Y. Kwak, J.-S. Park and Y.-J. Jeong, *J. Mater. Chem.*, 2001, 11, 1671-1674.
54. M. Ogawa and K. Kuroda, *Chem. Rev.*, 1995, 95, 399-438.
55. X. F. Liang, Y. B. Zang, Y. M. Xu, X. Tan, W. G. Hou, L. Wang and Y. B. Sun, *Colloid Surface A*, 2013, 433, 122-131.
56. R. Rojas, *Appl. Clay Sci.*, 2014, 87, 254-259.
57. R. Rojas, M. R. Perez, E. M. Erro, P. I. Ortiz, M. A. Ulibarri and C. E. Giacomelli, *Appl. Clay Sci.*, 2009, 331, 425-431.
58. Y. Chen and Y.-F. Song, *Ind. Eng. Chem. Res.*, 2013, 52, 4436-4442.
59. H. Nakayama, S. Hirami and M. Tsuhako, *J. Colloid Interface Sci.*, 2007, 315, 177-183.
60. N. Iyi, T. Matsumoto, Y. Kaneko and K. Kitamura, *Chem. Lett.*, 2004, 33, 1122-1123.
61. N. Iyi, T. Matsumoto, Y. Kaneko and K. Kitamura, *Chem. Mater.*, 2004, 16, 2926-2932.
62. S. L. Ma, L. Du, J. Wang, N. K. Chu, Y. H. Sun, G. B. Sun, X. J. Yang and K. Ooi, *Dalton Trans.*, 2011, 40, 9835-9843.
63. S. Miyata, *Clays and Clay Miner.*, 1983, 31, 305-311.
64. S. Miyata, *Clays and Clay Miner.*, 1975, 23, 369-&.
65. T. Yamaoka, M. Abe and M. Tsuji, *Mater. Res. Bull.*, 1989, 24, 1183-1199.
66. T. Nakato, K. Kuroda and C. Kato, *Chemistry of Materials*, 1992, 4, 128-132.
67. L. A. Vermeulen and M. E. Thompson, *Nature*, 1992, 358, 656-658.
68. Z. P. Liu, R. Z. Ma, M. Osada, N. Iyi, Y. Ebina, K. Takada and T. Sasaki, *J. Am. Chem. Soc.*, 2006, 128, 4872-4880.
69. M. Adachi-Pagano, C. Forano and J. P. Besse, *Journal of Materials Chemistry*, 2003, 13, 1988-1993.
70. G. J. Janz, J. W. Coutts, J. R. Downey and E. Roduner, *Inorganic Chemistry*, 1976, 15, 1755-1758.
71. X. B. Chen, X. D. Feng, J. Liu, G. E. Fryxell and M. L. Gong, *Separation Science and Technology*, 1999, 34, 1121-1132.
72. W. Yantasee, C. L. Warner, T. Sangvanich, R. S. Addleman, T. G. Carter, R. J. Wiacek, G. E. Fryxell, C. Timchalk and M. G. Warner, *Environ. Sci. Technol*, 2007, 41, 5114-5119.
73. C. Q. Liu, Y. Q. Huang, N. Naismith and J. Economy, *Environ. Sci. Technol*, 2003, 37, 4261-4268.
74. J. Liu, X. D. Feng, G. E. Fryxell, L. Q. Wang, A. Y. Kim and M. L. Gong, *Adv. Mater.*, 1998, 10, 161-+.
75. The acceptable limits of various elements for drinking water can be found in web site of U.S. Environmental Protection Agency (E.P.A.) http://www.epa.gov/safewater/contaminants/index.html.
76. M. Draganjac, E. Simhon, L. T. Chan, M. Kanatzidis, N. C. Baenziger and D. Coucouvanis, *Inorg. Chem.*, 1982, 21, 3321-3332.
77. D. Coucouvanis, P. R. Patil, M. G. Kanatzidis, B. Detering and N. C. Baenziger, *Inorg. Chem.*, 1985, 24, 24-31.

Table 1. Chemical compositions of LDH samples with different interlayer anions.

Samples	d_{basal} / nm	Chemical Formula	Wt %, Found (Calcd.) Mg	Al	C	H	N
CO_3–LDH	0.76	$Mg_{0.66}Al_{0.34}(OH)_2(CO_3)_{0.17}\cdot 0.8H_2O$	19.69 (19.55)	11.63 (11.55)	2.43 (2.57)	4.53 (4.50)	–
NO_3–LDH	0.89	$Mg_{0.66}Al_{0.34}(OH)_2(NO_3)_{0.32}(CO_3)_{0.01}\ 0.6H_2O$	18.94 (18.27)	11.28 (10.43)	0.18 (0.14)	3.59 (3.84)	4.62 (4.45)
S_4–LDH	0.81	$Mg_{0.66}Al_{0.34}(OH)_2(S_4)_{0.13}(NO_3)_{0.01}(CO_3)_{0.04}\ 0.8H_2O$	16.72 (17.02)	10.26 (9.90)	0.49 (0.52)	3.84 (3.87)	0.11 (0.15)
S_2–LDH	0.80	$Mg_{0.66}Al_{0.34}(OH)_2(S_2)_{0.14}(NO_3)_{0.01}(CO_3)_{0.02}\ 0.8H_2O$	17.25 (18.04)	10.31 (10.50)	0.29 (0.27)	3.97 (4.56)	0.15 (0.16)

Table 2. Adsorption results of S_4-LDH toward eight metal ions (10 ppm). [a]

S_4-LDH	Initial solution		After 3h adsorption		M^{n+} removal (%)	K_d (ml/g)
single ion	C_0 (ppm)	pH	C_f (ppm)	pH		
Co	9.775	5.14	8.943	5.42	8.5	80
Ni	9.714	5.20	9.208	5.37	5.2	47
Cu	10.097	4.68	2.661	5.60	73.6	2.4×10^3
Zn	8.877	4.92	6.543	5.37	26.3	305
Ag	10.234	4.40	0.001	5.70	100.0	8.8×10^6
Pb	8.464	4.74	1.867	5.58	77.9	3.0×10^3
Cd	9.903	4.97	6.771	5.19	31.6	396
Hg	7.802	2.78	0.0008	3.27	100.0	8.4×10^6

[a] ion concentration: ~10 ppm per ion.

V, 30 ml; m (mass of solid sample), 0.035 g; V/m ratio: 30/0.035 = 860.

Contact time: 3 h.

Table 3. Adsorptive selectivity toward mixed ions (10 ppm per ion) using different amounts of S_4-LDH. [a]

S_4-LDH	Mixed ions	Co	Ni	Cu	Zn	Ag	Pb	Cd	Hg
	C_0 (ppm)	10.62	11.01	11.08	10.57	11.45	11.34	8.01	9.82
0.002 g	C_f-3h (ppm)	10.61	11.00	8.85	10.47	0.40	11.30	7.61	0.42
	Ion capacity (mg/g)	0.15	0.15	33.45	1.50	165.8	0.60	6.00	141
	Removal (%)	0.09	0.09	20.13	0.95	96.51	0.35	4.99	95.72
	K_d (ml/g)	14	14	3.8×10^3	143	4.1×10^5	53	788	3.3×10^5
	Selectivity order	Cu < Ag, Hg							
0.005 g	C_f-3h (ppm)	10.60	10.99	2.22	10.42	0.001	8.82	6.85	0.001
	Ion capacity (mg/g)	0.1	0.1	53.2	0.9	68.7	15.1	7.0	59
	Removal (%)	0.19	0.18	79.96	1.42	99.99	22.22	14.48	99.99
	K_d (ml/g)	11	11	2.4×10^3	86	6.8×10^7	1.7×10^3	1.0×10^3	5.9×10^7
	Selectivity order	Cd, Pb < Cu < Ag, Hg							
0.01 g	C_f-3h (ppm)	10.60	10.98	0.008	8.51	0.001	0.096	0.010	0.001
	Ion capacity (mg/g)	0.06	0.09	33.2	6.2	34.3	33.7	24.0	29.4
	Removal (%)	0.19	0.27	99.93	19.49	99.99	99.15	99.88	99.99
	K_d (ml/g)	6	8	4.1×10^6	726	3.4×10^7	3.5×10^5	2.4×10^6	2.9×10^7
	Selectivity order	Cd, Pb < Cu < Ag, Hg							
0.02 g	C_f-3h (ppm)	10.16	10.61	0.002	0.071	0.001	0.010	0.006	0.0008
	Ion capacity (mg/g)	0.7	0.6	16.6	15.7	17.2	17.0	12.0	14.7
	Removal (%)	4.33	3.63	99.98	99.33	99.99	99.91	99.93	99.99
	K_d (ml/g)	68	57	8.3×10^6	2.2×10^5	1.7×10^7	1.7×10^6	2.0×10^6	1.8×10^7
	Selectivity order	Zn < Cd, Pb < Cu < Ag, Hg							
0.035 g	C_f-3h (ppm)	9.35	10.16	0.001	0.007	0.001	0.006	0.001	0.0007
	Ion capacity (mg/g)	1.1	0.7	9.5	9.1	9.8	9.7	6.9	8.5
	Removal (%)	11.96	7.72	99.99	99.93	99.99	99.95	99.99	99.99
	K_d (ml/g)	116	72	9.5×10^6	1.3×10^6	9.8×10^6	1.6×10^6	6.9×10^6	1.1×10^7
	Selectivity order	Ni, Co << Zn < Pb < Cd < Cu < Ag, Hg							

[a] ion concentration: ~10 ppm each cation.

V: 30 ml, m (mass of solid sample): 0.002 g - 0.035 g.

The V/m ratios are 860, 1500, 3000, 6000, 15000, respectively.

Contact time: 3 h.

Table 4. Selective adsorption results of S_x-LDH for the separation of Ag^+ from Hg^{2+}. [a]

S_4-LDH	0.001 g		0.002 g	
	Ag^+	Hg^{2+}	Ag^+	Hg^{2+}
C_0 (ppm)	21.8	17.5	21.8	17.5
C_f - 6h (ppm)	20.2	4.03	4.51	1.50
K_d - 6h (ml/g)	2.3×10^3	1.0×10^5	5.7×10^4	1.5×10^5
pH - 6h	2.84 → 4.46		2.84 → 4.65	

S_2-LDH	0.001 g		0.002 g	
	Ag^+	Hg^{2+}	Ag^+	Hg^{2+}
C_0 (ppm)	21.8	17.5	21.8	17.5
C_f - 6h (ppm)	20.6	5.76	8.86	1.73
K_d - 6h (ml/g)	1.7×10^3	6.1×10^4	2.1×10^4	1.4×10^5
pH - 6h	2.84 → 4.22		2.84 → 4.57	

[a] 30 ml solution of $Hg(NO_3)_2$ and $AgNO_3$, 20 ppm concentration per ion.

Table 5. Adsorptive capacity toward individual metal ions (10 mM) by S_2-LDH. [a]

	C_0		C_f - 3d		ion capacity		Removal (%)	K_d
Ions	mM	ppm	mM	ppm	mg/g	mmol/g		
Co^{2+}	8.93	526.21	6.10	359.53	83	1.40	31.7	232
Ni^{2+}	10.15	595.69	5.92	347.39	106	1.80	41.7	357
Cu^{2+}	9.69	615.38	5.01	318.52	127	2.01	48.2	466
Zn^{2+}	9.40	614.76	4.96	324.19	145	2.22	47.3	448
Ag^+	7.11	766.52	0.001	0.11	383	3.55	100	3×10^6
Pb^{2+}	9.47	1961.56	5.18	1072.88	483	2.33	45.3	414
Cd^{2+}	9.51	1068.92	8.15	916.28	57	0.50	14.3	83
Hg^{2+}	10.89	2184.94	4.06	813.43	686	3.42	62.8	843

[a] ~individual solutions each containing Co^{2+}, Ni^{2+}, Cu^{2+}, Zn^{2+}, Ag^+, Pb^{2+}, Cd^{2+}, Hg^{2+} with a 10 mM concentration.
V, 10 ml; m, 0.02 g; V/m ratio, 10 / 0.02 = 500.
Contact time: 3d.

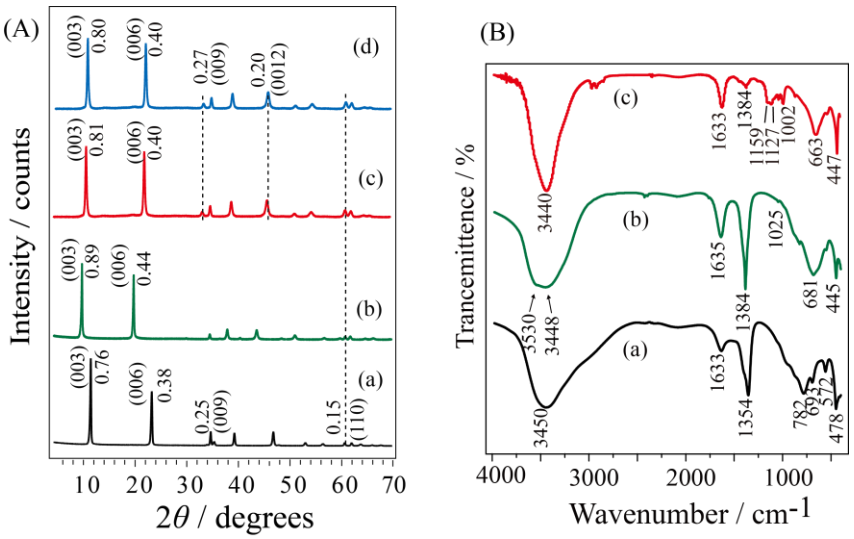

Fig. 1 (A) XRD patterns of (a) CO_3–LDH, (b) NO_3–LDH, (c) S_4–LDH and (d) S_2–LDH (The *d*-values are given in nanometers); and (B) FT-IR spectra of (a), (b) and (c).

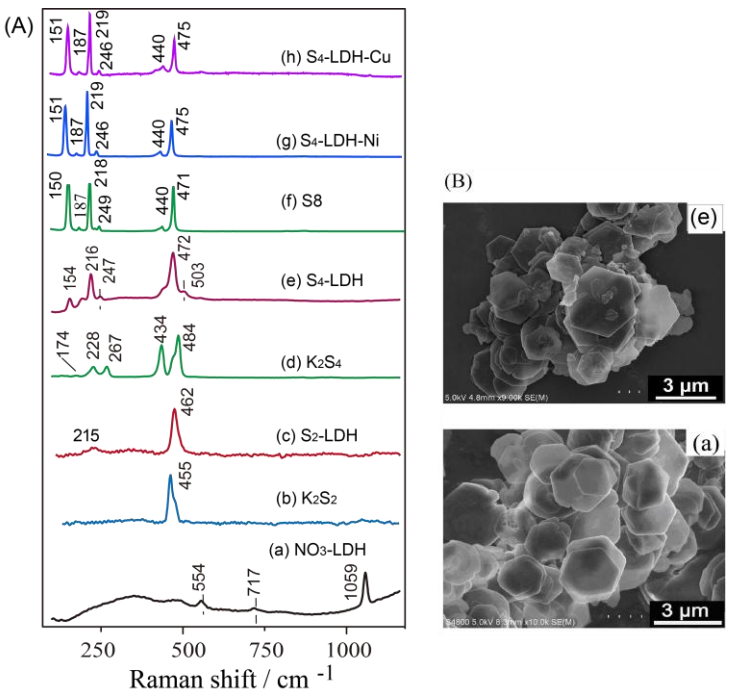

Fig. 2 (A) Raman spectra of (a) NO_3–LDH, (b) K_2S_2, (c) S_2–LDH, (d) K_2S_4, (e) S_4–LDH, (f) S_8, and after S_4–LDH adsorbed (g) Ni^{2+} and (h) Cu^{2+} of 10 ppm concentration; (B) SEM images of (a) and (c).

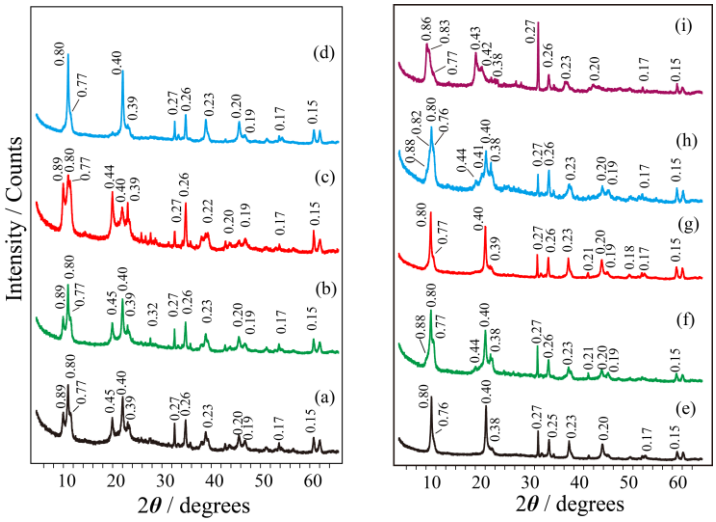

Fig. 3 XRD patterns of samples obtained after 0.035 g S_4-LDH adsorbed metal ions of (a) Co^{2+}, (b) Ni^{2+}, (c) Cu^{2+}, (d) Zn^{2+}, (e) Ag^{+}, (f) Pb^{2+}, (g) Cd^{2+}, (h) Hg^{2+} and (i) their mixed solution (concentration of each ion, 10 ppm).

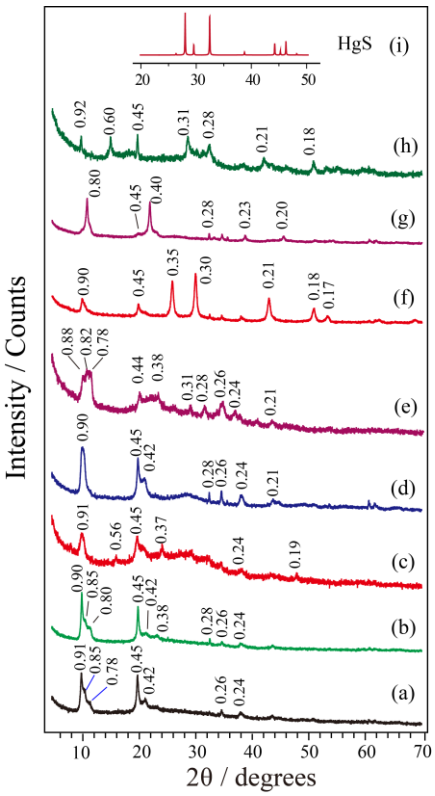

Fig. 4 XRD patterns of samples obtained after 0.02 g S_2-LDH adsorbed metal ions of (a) Co^{2+}, (b) Ni^{2+}, (c) Cu^{2+}, (d) Zn^{2+}, (e) Ag^{+}, (f) Pb^{2+}, (g) Cd^{2+}, (h) Hg^{2+}, (concentration of each ion, 10 mM) and (i) the standard pattern of HgS.

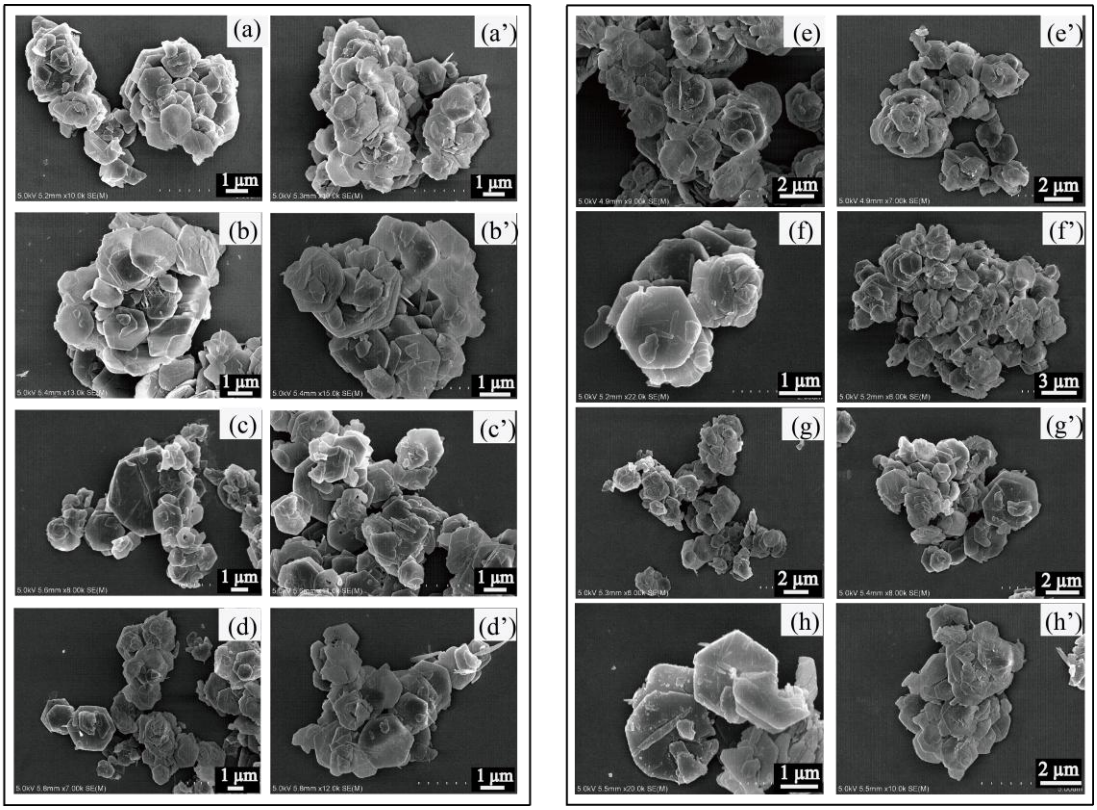

Fig. 5 SEM images of solid samples after 0.035 g S_4-LDH adsorbed ions of (a, a') Co^{2+}, (b, b') Ni^{2+}, (c, c') Cu^{2+}, (d, d') Zn^{2+}, (e, e') Ag^{+}, (f, f') Pb^{2+}, (g, g') Cd^{2+}, and (h, h') Hg^{2+} (10 ppm concentration).

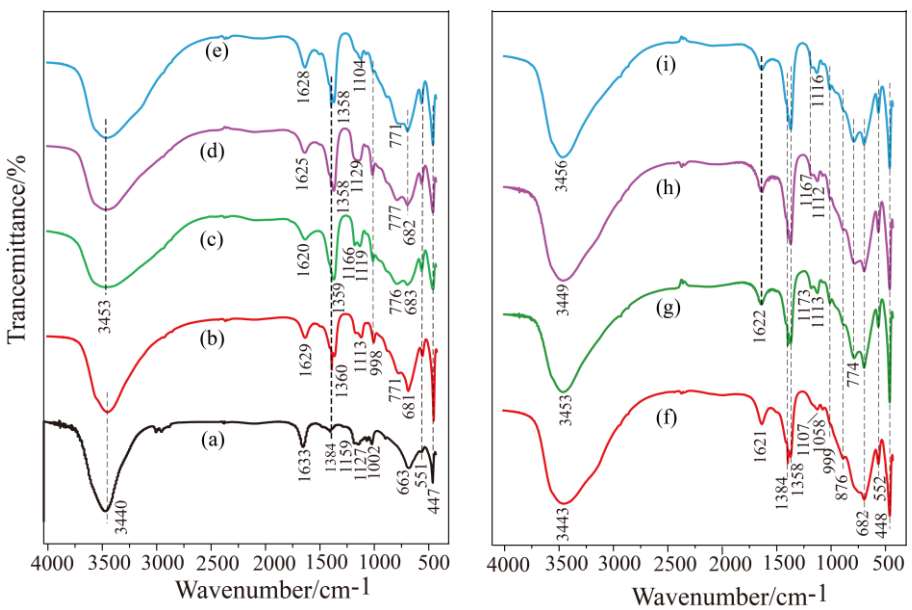

Fig. 6 IR spectra of (a) pristine S_4-LDH and after it adsorbed metal ion of (b) Co^{2+}, (c) Ni^{2+}, (d) Cu^{2+}, (e) Zn^{2+}, (f) Ag^{+}, (g) Pb^{2+}, (h) Cd^{2+} and (i) Hg^{2+} (10 ppm concentration).

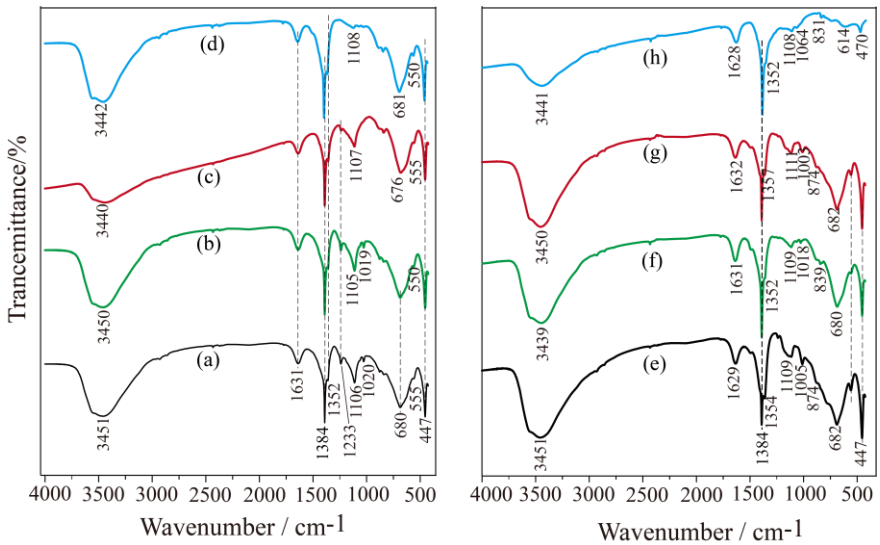

Fig. 7 IR spectra of samples after S_4-LDH adsorbed ions of (a) Co^{2+}, (b) Ni^{2+}, (c) Cu^{2+}, (d) Zn^{2+}, (e) Ag^{+}, (f) Pb^{2+}, (g) Cd^{2+} and (h) Hg^{2+}. (concentration, 10 mM ions)

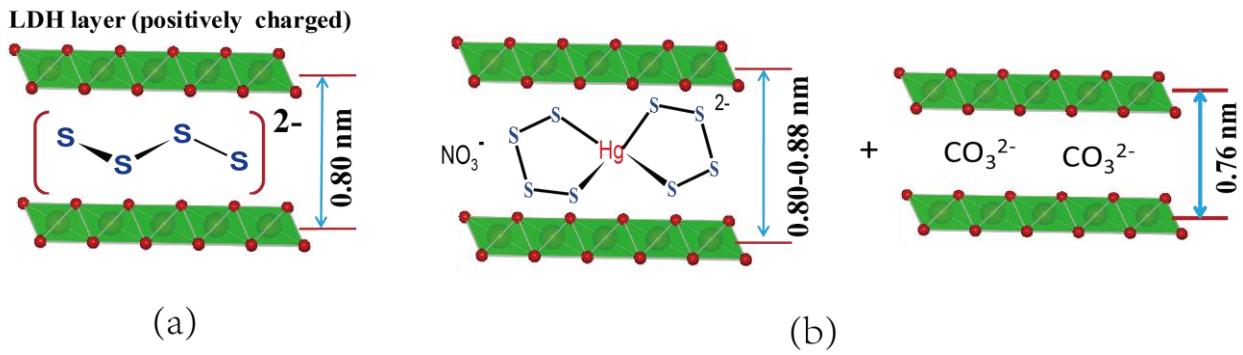

Scheme 1. Arrangement of (a) polysulfide $[S_4]^{2-}$ group in S_4-LDH, (b) proposed metal binding in the interlayer space and formation of CO_3-LDH.

Graphical Abstract

Highly Selective and Efficient Heavy Metal Capture with Polysulfide Intercalated Layered Double Hydroxides

Shulan Ma, Qingmei Chen, Hao Li, Pengli Wang, Saiful M. Islam, Qingyang Gu, Xiaojing Yang, Mercouri G. Kanatzidis*

Intercalation of polysulfides into LDHs forms layered composites that can separate Hg^{2+}, Ag^{+} and Cu^{2+} from mixed ions with high selectivity and capacity.